INTEGRATED NUMERICAL AND EXPERIMENTAL INVESTIGATION OF ACTUATOR PERFORMANCE FOR GUIDANCE OF SUPERSONIC PROJECTILES

Sidra I. Silton*
U.S. Army Research Laboratory
Aberdeen Proving Ground, MD 21005

Kevin C. Massey
Georgia Tech Research Institute
Smyrna, GA 30080

ABSTRACT

A recent study showed that the complex 3-D shock/boundary layer interaction of a pin placed next to a fin produces an asymmetric lift force that can be utilized for flight control of a projectile. The current study was completed to validate this new technology. A similar projectile was modeled, using high performance fluid dynamic computations and six degree-of-freedom trajectory simulations, to determine the projectile's flight characteristics prior to being flown in the US Army Research Laboratory's Aerodynamic Experimental Facility. A flight test was designed using this asymmetric lift to produce roll torque. Analysis of the flight data determined that the projectiles with pins developed the expected rolling moments. Computations were completed after the range test on the experimental model for computational validation.

1. INTRODUCTION

The defense community has recently been interested in guided projectiles that operate in the high supersonic to hypersonic range for various missions. One scenario for missile defense assumes that medium caliber guns (35 mm to 75 mm) with high rates of fire could launch multiple supersonic projectiles that could be guided into an incoming missile. For military programs that plan to utilize high speed guided munitions, large turning forces may be necessary due to the high closure rates between the projectile and an agile, maneuverable target.

The program discussed herein was conducted as an initial feasibility study for the use of strategically located actuators to provide the necessary turning force to terminally steer a Defense Advanced Research Project Agency (DARPA) command-guided, medium caliber projectile. The actuators were designed to use supersonic adaptive flow control to enhance the divert force generation. Recent studies at Georgia Tech Research Institute (GTRI) (Massey et al., 2004) have found that the introduction of pins† on a projectile in the vicinity of the fins creates shock patterns that impinge on both the fin and body surfaces. The forces created by the shock impingement are capable of providing control forces through asymmetric lift.

The effort presented here was conducted to model and validate that placement of pins next to the fins does indeed produce asymmetric lift. Specifically, it was desired to determine if the lift capability of the adaptive flow control technique can be used to create roll torque using two diametrically opposed pins. The creation of sufficient roll torque would produce measurable projectile rotation that can be measured in an aeroballistic facility. The current effort consisted of three parts:

1. high performance computations to predict projectile behavior due to the presence of the pins for adaptive flow control;
2. an experimental program in an aeroballistic range to determine the asymmetric lift produced by the adaptive flow control technique; and
3. comparison of experimental and computational results for future use.

2. BLIND SIMULATIONS

Blind simulations (computational fluid dynamics (CFD) and six degree-of-freedom (6-DOF) simulations) were completed prior to experimental range tests to determine expected flight characteristics of the projectile.

2.1 Computational Fluid Dynamics

CFD simulations were completed using CFD++ (Metacomp Technologies, 2000) to obtain force and moment data for the projectiles over a range of supersonic Mach numbers. CFD++ solves the Reynolds-averaged Navier-Stokes equations within a finite volume framework. The pointwise k-ε turbulence model (Goldberg et al., 1998) was used for the computation of the turbulent flow. Spatial discretization is accomplished using the cell face normal at the cell face centroid, which

† The use of these pins or similar pins to produce steering forces and moments is a proprietary technology developed by the Georgia Tech Research Institute and is protected under US Patent Law. Used with permission. Patent Pending.

Report Documentation Page

Form Approved
OMB No. 0704-0188

1. REPORT DATE	2. REPORT TYPE	3. DATES COVERED
00 DEC 2004	**N/A**	**-**

4. TITLE AND SUBTITLE	5a. CONTRACT NUMBER
Integrated Numerical And Experimental Investigation Of Actuator Performance For Guidance Of Supersonic Projectiles	5b. GRANT NUMBER
	5c. PROGRAM ELEMENT NUMBER
6. AUTHOR(S)	5d. PROJECT NUMBER
	5e. TASK NUMBER
	5f. WORK UNIT NUMBER
7. PERFORMING ORGANIZATION NAME(S) AND ADDRESS(ES) **U.S. Army Research Laboratory Aberdeen Proving Ground, MD 21005; Georgia Tech Research Institute Smyrna, GA 30080**	8. PERFORMING ORGANIZATION REPORT NUMBER
9. SPONSORING/MONITORING AGENCY NAME(S) AND ADDRESS(ES)	10. SPONSOR/MONITOR'S ACRONYM(S)
	11. SPONSOR/MONITOR'S REPORT NUMBER(S)

12. DISTRIBUTION/AVAILABILITY STATEMENT
Approved for public release, distribution unlimited

13. SUPPLEMENTARY NOTES
See also ADM001736, Proceedings for the Army Science Conference (24th) Held on 29 November - 2 December 2005 in Orlando, Florida. , The original document contains color images.

14. ABSTRACT

15. SUBJECT TERMS

16. SECURITY CLASSIFICATION OF:			17. LIMITATION OF ABSTRACT	18. NUMBER OF PAGES	19a. NAME OF RESPONSIBLE PERSON
a. REPORT	b. ABSTRACT	c. THIS PAGE			
unclassified	**unclassified**	**unclassified**	**UU**	**22**	

Standard Form 298 (Rev. 8-98)
Prescribed by ANSI Std Z39-18

is obtained by reconstructing the cell centroid values. The point-implicit integration scheme was used to solve the steady-state simulation.

The full scale 50 mm projectile with a tapered leading and trailing fin edge and sharp nose tip was modeled (Fig. 1a). In order to determine the effect of the control pins on the drag coefficient, simulations were completed on three geometries: a projectile with no control pins (baseline), a projectile with diametrically opposed rectangular control pins, and a projectile with diametrically opposed parallelogram shaped (trapezoidal) control pins (Fig. 1b). These control pins were turned at a 30° angle and placed parallel to the fins. The pin shapes and placement correspond to those optimized by GTRI for which limited CFD data had previously been obtained (Massey et al., 2004).

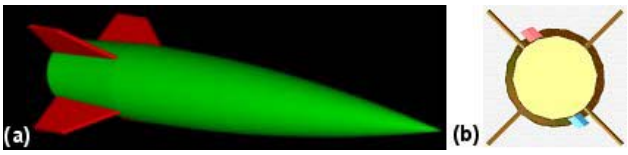

Fig. 1: (a) 3-D rendering of baseline CFD model and (b) aft view of pins.

The numerical grids for each of these geometries were supplied by Metacomp Technologies under contract from GTRI. Each grid was unstructured and contained mostly hexahedral cells, with a small number of triangular prisms and contained approximately 2.9 millions cells.

The far field boundary condition is set to allow the solver to determine the conditions at the far field boundary (inflow, subsonic outflow or supersonic outflow) and either explicitly sets the boundary condition to free stream conditions (inflow, subsonic outflow) or extrapolates as necessary (supersonic outflow). Free stream pressure and temperature are set to standard sea level conditions (i.e. 101.325 kPa and 288.15 K, respectively). Density is then calculated from the perfect gas assumption. Velocity is varied between Mach 1.5 and 4.0 and angle-of-attack is fixed at zero degrees. For the projectile body, fins, and control pins, the boundary condition is set to be a no-slip, adiabatic wall.

2.2 Six Degree-of-Freedom Trajectory Simulations

6-DOF simulations were completed using the PRODAS (ArrowTech Associates, 2001) 6-DOF fixed plane trajectory simulation to determine the number of revolutions the projectile could be expected to complete as it flew down the 100-m aeroballistic range. The physical characteristics of the projectile were specified within PRODAS and a database of aerodynamic coefficients as a function of Mach number was used. For the blind simulations, the database consisted of augmented results from a previously completed flight test using a half scale 25-mm (baseline) projectile (Fig. 2) launched from a rifled barrel (Whyte et al., 2002). The augmentation was the change in axial force and rolling moment coefficients due to the presence of the control pins as obtained from CFD.

Fig. 2: Baseline 25-mm projectile as also used in previously completed flight test (Whyte et al., 2002).

Initial conditions are specified for the gun and the projectile during setup of the 6-DOF simulation. The gun is set to have an elevation of 0.001° and no azimuth. Standard sea level meteorological conditions are used. The gun twist is made extremely large so that the spin at the muzzle is 0 Hz (i.e. smooth bore gun). The initial projectile velocity was varied between Mach 2.0 and Mach 3.0 to match the expected range Mach numbers. The projectile starts at the coordinate system origin with no pitch angle, pitch rate, or yaw angle. The initial yaw rate was set to −15.0 rad/sec, as this is a typical value for small caliber projectiles. Once the equations of motion are initialized, a fourth order Runge-Kutta numerical integration scheme is used to integrate the equation of motions in time. The time step is dynamically chosen in order to account for both pitch frequencies (usually 20 time steps per yaw cycle).

3. RANGE TESTS

After completion of the blind simulations, flight hardware was designed and built. The baseline projectile was a 25 mm sub-scale projectile (Whyte et al, 2002) with blunt fin leading and trailing edges, a relatively large fillet between the fins and the body and a blunt nose tip (Fig. 2). A steel spin pin was inserted in the projectile base to determine the projectile roll position during analysis. The roll torque models (Fig. 3) were created using a control pin of circular cross-section rather than that of the optimized parallelogram shape investigated in the computer simulations to ease machining requirements on a proof of concept experiment. The cylindrical control pins were constructed of $1/16^{th}$ inch diameter drill rod and machined to 15.0 mm and 16.7 mm in length to produce the 1.78-mm short control pin model and the 2.54-mm long control pin model, respectively. A hole was drilled through the body to allow for the correct placement of the diametrically opposed control pins (approximately

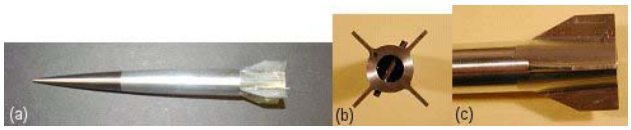

Fig. 3: Photo of short pin model (a) complete projectile, (b) base view, and (c) close-up of fins.

2.79 mm from the projectile base and a 16° rotation from the fin). The chosen rod was fit through the predrilled hole and centered to create two equal length control pins.

In order to complete the range test, the projectile was encased in a sabot system for launch. The sabot system consisted of four sabot petals, the pusher, and the obturator (Fig. 4). The four sabot petals and the obturator/pusher cup were manufactured from nylon. The pusher was manufactured from 17-4 stainless steel. Each of the four sabot petals had two slots cut out for the fins and control pins. The petals were internally contoured to the projectile shape and fit together to create a cylinder. The pusher cup accommodated the pusher, the sabot petals, and the projectile. The exterior diameter of the pusher cup was flared near the base for an interference fit with the barrel. This allowed for a consistent velocity to be maintained for the charge weight utilized. The total package weight (projectile and sabot system) was approximately 120g.

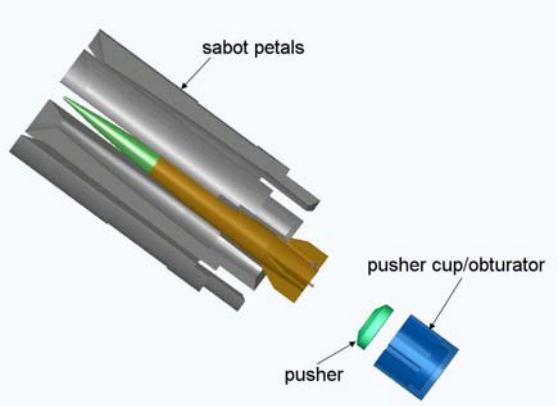

Fig. 4: Exploded 3-D rendering of the sabot system with projectile.

The projectiles were fired from a modified, smooth bore, 25-mm Bushmaster Mann barrel through the range at the US Army Research Laboratory (ARL) Aerodynamic Experimental Facility (AEF). The ARL AEF was designed to evaluate the complete aeroballistics of projectiles as described by Braun (Braun, 1958). Up to six high power, orthogonal x-rays were utilized to determine the structural integrity and launch dynamics of the projectile in a manner consistent with other programs (Plostins et al., 1989; Plostins et al., 1991; Bornstein et al., 1992). The range facility itself consists of 39 orthogonal spark shadowgraph stations (Fig. 5) arranged in 5 groups over 100 m of trajectory length. Each station provides a vertical and horizontal direct shadow image of the passing projectile at a known time. From these images, the raw data (i.e., the spatial coordinates and angular orientation of the projectile relative to the earth fixed range coordinate system as a function of the spark time) can be obtained.

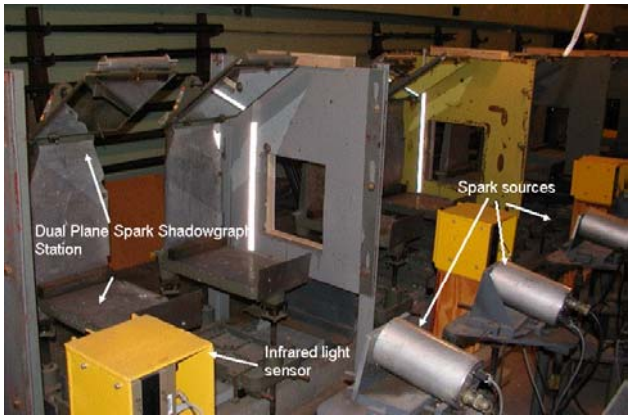

Fig. 5: Photo of dual plane (orthogonal) spark shadowgraph stations with infrared sensor triggers and spark source.

The raw data is processed with ARFDAS (ArrowTech Associates, 1997) to determine the aerodynamic coefficients and derivatives. ARFDAS incorporates a standard linear theory analysis and a 6-DOF numerical integration technique. The 6-DOF routine incorporates the maximum likelihood method (MLM) to match the theoretical trajectory to the experimentally measured trajectory. The MLM is an iterative procedure that adjusts the aerodynamic coefficients to maximize a likelihood function. Each projectile fired was initially analyzed separately (single fits), then combined in appropriate groups for simultaneous analysis using the multiple fit capability. The multiple fit approach provided a more complete spectrum of angular and translational motion than would be available from any single trajectory.

4. RESULTS

4.1 Blind Simulations

Completing the CFD simulations between Mach 1.5 and Mach 4.0 insured data overlap with the previously obtained experimental data (Whyte et al., 2002). As the CFD data necessary to augment the experimental data for use in the 6-DOF simulations was the increase in drag due to the presence of the control pins and the roll torque created by the control pins, only 0° angle-of-attack was considered.

The drag was determined directly from the axial force coefficient, C_{X0}. The presence of the control pins increased the drag over the entire range of Mach number, as expected (Fig. 6). At a given Mach number, the increase in drag due to the presence of the control pins decreased with increasing Mach numbers.

The roll torque was directly determined from the axial moment. Fig. 7 shows the surface pressure contours

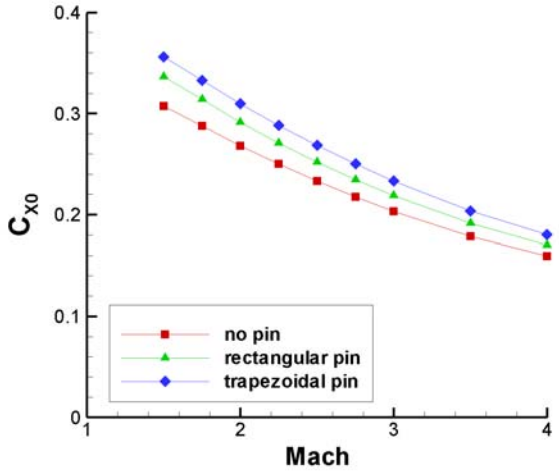

Fig. 6: Computed axial force coefficient vs. Mach number.

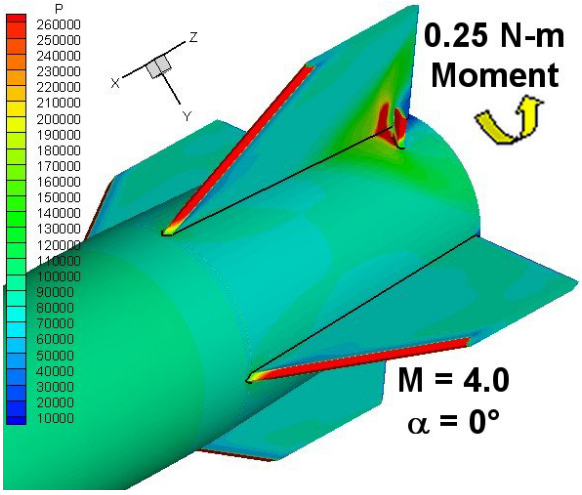

Fig. 7: Surface pressure contours, blind CFD.

for the projectile with rectangular cross section control pins. The areas of high pressure on the fins near the control pins cause the roll torque development. Fig. 8 shows that the roll torque coefficient ($C_{l\delta}$) decreased by almost 75% over the range of Mach numbers investigated. As expected, the trapezoidal control pin created substantially more roll torque over the entire range of Mach numbers.

After completing the CFD for both the rectangular pin and the trapezoidal pin configurations, it was believed that the rectangular pin data would likely be more in line with that of the cylindrical control pins in the planned range test. Hence, the aerodynamic coefficients from the rifled range test (Whyte et al., 2002) were modified by the CFD results of the rectangular control pins.

The 6-DOF simulations were completed at Mach 2.0, 2.5, and 3.0 corresponding to the Mach numbers of the planned range test. The results showed that the projectile

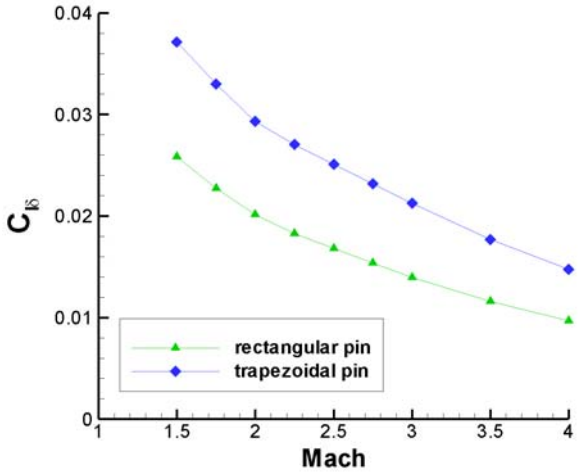

Fig. 8: Computed roll torque coefficient vs. Mach number.

could be expected to complete 8 to 10 turns during the flight down range depending on Mach number.

4.2 Range Test

Up to three Mach numbers were investigated for each configuration for a total of 15 shots. For the baseline configuration, one projectile was shot for each nominal Mach number of 2.0, 2.5, and 3.0. For the short pin model, three projectiles were shot for each nominal Mach number of 2.0, 2.5, and 3.0. For the long pin model, three projectiles were shot for the nominal Mach number of 3.0.

Gun launch was successful: consistent velocities were obtained, the sabot petals cleanly separated upon muzzle exit – there was no interference with the projectile motion, and structural integrity of the projectile was maintained. Horizontal and vertical shadowgraph photographs were obtained at each station for each shot. Thus, all aerodynamic coefficients were obtained for each shot. Only the results of C_{X0} and $C_{l\delta}$, and the resulting travel down range are presented here for brevity and comparison with CFD. The reader is referred to (Silton, 2004) for the remaining aerodynamic coefficients.

C_{X0} decreased nearly linearly with Mach number for both the baseline and short pin configuration (Fig. 9). For a given Mach number, C_{X0} increased with the introduction of the control pin as well as with pin length.

The diametrically opposed control pins created roll torque as expected (Fig. 10). The non-zero $C_{l\delta}$ for the baseline case can be accounted for small asymmetries due to the spin pin. For the short pin geometry, $C_{l\delta}$ does not significantly vary with Mach number unlike the other aerodynamic coefficients. At Mach 3, the 50% increase in control pin length nearly doubled the roll torque coefficient. This indicates that there would be a much faster response from the projectile.

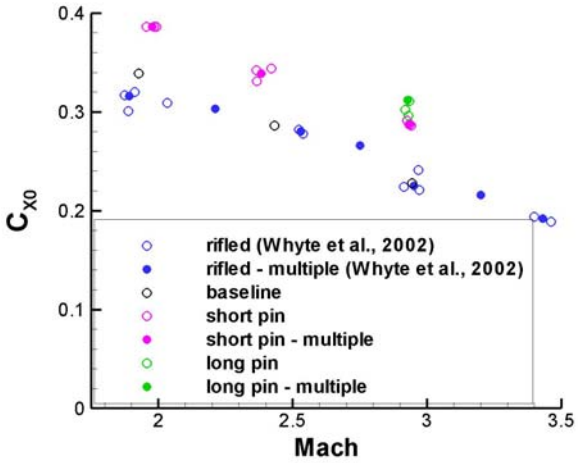

Fig. 9: Experimental zero-yaw axial force coefficient as a function of Mach number.

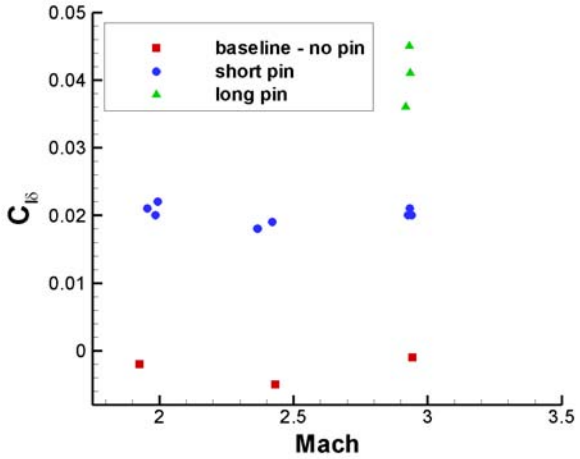

Fig. 10: Experimental roll torque coefficient as a function of Mach number.

The roll rate increased as the projectile traveled down range. Comparing shadowgraphs at adjacent stations when the roll rate is small (Fig. 11) and further down range when a larger roll rate has been achieved (Fig. 12), the difference is quite noticeable. The spin pin has barely moved between Fig. 11(a) and (b), where the round traveled from 6.7 m to 8.2 m. At least a 90° rotation was achieved between Fig. 12(a) and (b), where the round traveled from 90 m to 91.4 m. Although not shown here, the difference in Mach number does not much effect the roll rate. The increase in pin length, however, more than doubles the roll rate by the end of the range.

4.3 Simulation and Range Test Comparisons

In this subsection, the results of the range test are compared to:

1. the blind CFD and 6-DOF simulations;
2. 6-DOF simulations using updated aerodynamics coefficients; and
3. CFD results using matched physical and atmospheric conditions.

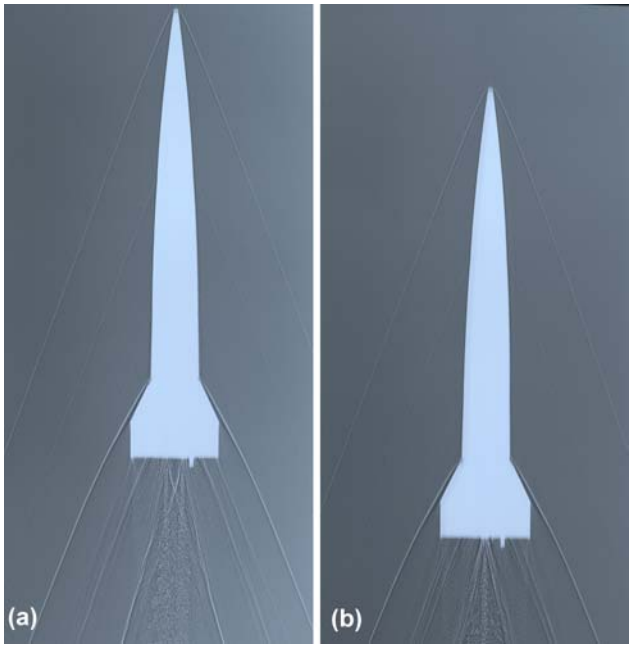

Fig. 11: Vertical shadowgraphs for shot 24096 at stations (a) 22 and (b) 27.

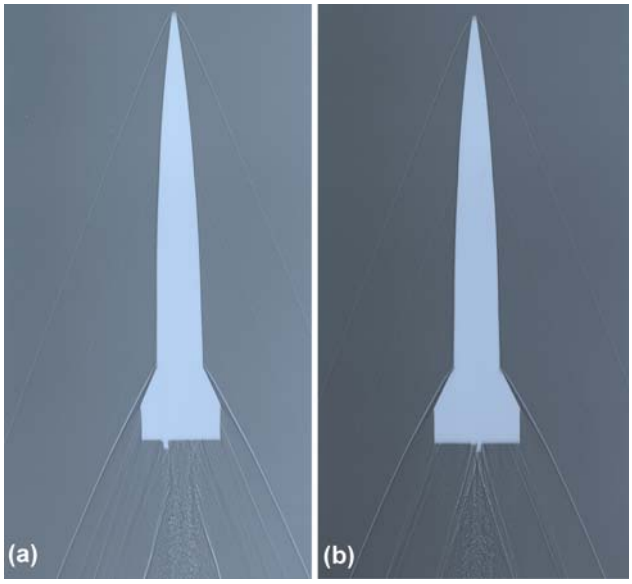

Fig. 12: Horizontal shadowgraphs for shot 24096 at stations (a) 295 and (b) 300.

4.3.1 Blind CFD and 6-DOF

This comparison was completed in order to determine how well the blind CFD and 6-DOF simulations predicted the range test results despite differences in the geometric model. The differences were not just model size, but also fin leading and trailing edge taper (tapered vs. blunt), nose bluntness (sharp vs. blunt) and control pin shape (rectangular vs. cylindrical) and relative orientation (parallel vs. radial to the fin). Also, the 6-DOF simulations assumed aerodynamic coefficients determined for the baseline projectile shot from a rifled gun tube (Whyte et al., 2002).

A larger C_{X0} is expected for the range test due to the bluntness of the fins and the nose tip. Nonetheless, CFD does a reasonable job of predicting C_{X0} (Fig. 13). CFD underpredicts the increase in C_{X0} due to the presence of the control pin due to the difference in pin shape. However, augmenting the rifled range test data by this difference produces a fair estimate of C_{X0} for the short pin projectile.

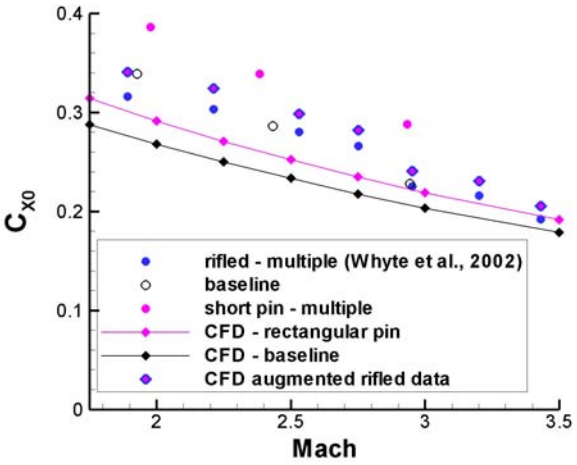

Fig. 13: Axial force coefficient comparison between range test and blind CFD.

CFD does well predicting $C_{l\delta}$ despite modeling rectangular, rather than the experimental cylindrical, pins (Fig. 14). The predictions are quite good at Mach 2.0 and 2.5 leading one to believe that the differences in control pin shape are insignificant at these Mach numbers. Perhaps the 3-D relieving effects are as significant for the rectangular pins turned at a 30° angle and parallel to the fins as for the symmetrically placed circular pins (Massey et al., 2004). At Mach 3.0, $C_{l\delta}$ is noticeably underpredicted indicating that geometric differences and pin placement become important at higher Mach numbers.

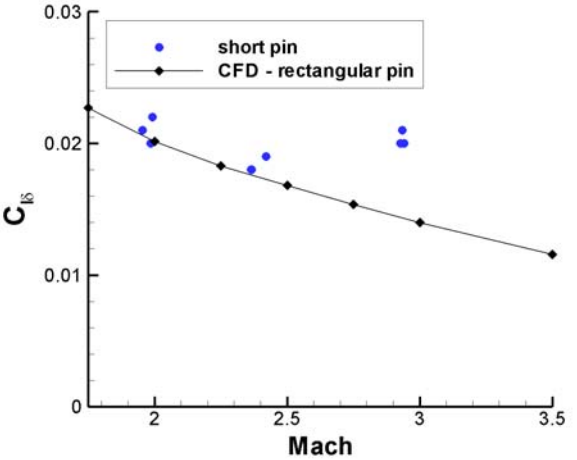

Fig. 14: Roll torque coefficient comparison between range test and blind CFD.

As there were differences between the axial force, and roll torque coefficients used for the 6-DOF simulation and the values determined by the range test, one expects there to be corresponding differences in the results. This was indeed the case as the number of revolutions achieved at Mach 3.0 was underpredicted at 90 m (8.7 versus 7.3) while the number of revolutions at the lower Mach numbers was overpredicted at 90 m (6.8 versus 7.9 at Mach 2.5 and 7.0 versus 8.5 at Mach 2.0). Regardless, the blind 6-DOF simulations provided a good idea of what could be expected to occur during the range tests.

4.3.2 Updated 6-DOF

After completion of the range tests, the 6-DOF simulations were repeated using the aerodynamic coefficients obtained from the range test to populate the database. Very good agreement in both roll rate and, hence, number of revolutions was achieved (Fig. 15) indicating that accurate 6-DOF simulations can be obtained if an accurate aerodynamic coefficient database is available.

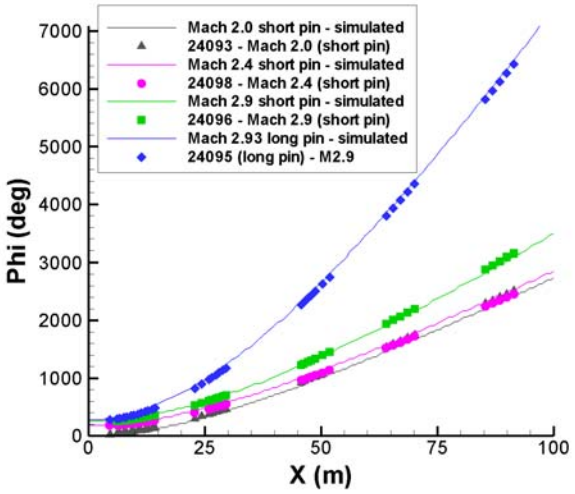

Fig. 15: Comparison of updated 6-DOF and range test results for projectile rotation as a function of distance.

4.3.3 Updated CFD

After completion of the range tests, two new sets of CFD calculations were completed by Metacomp Technologies using the short cylindrical pin model and the long cylindrical pin model. Each computation was completed at 0° angle-of-attack and exactly matched the test conditions of the multiple fit range results for the model allowing for direct comparison of C_{X0} and $C_{l\delta}$.

CFD accurately determined C_{X0} at all three Mach numbers for both model configurations (Fig. 16). CFD did not do quite as well predicting $C_{l\delta}$ (Fig. 17). CFD predicted a continuous decrease for the short pin model. The range test, however, showed a small decrease in $C_{l\delta}$

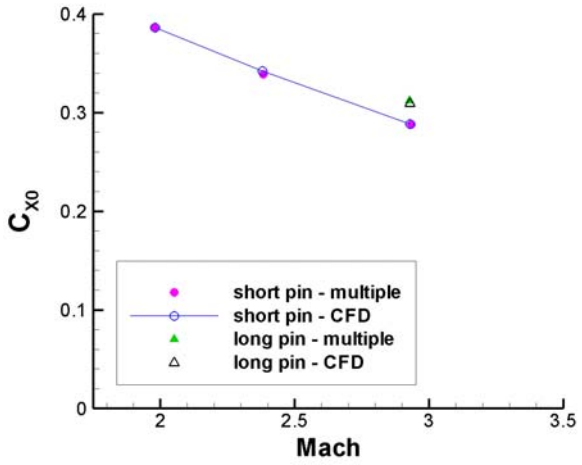

Fig. 16: Comparison of updated CFD to range test zero-yaw axial force coefficient.

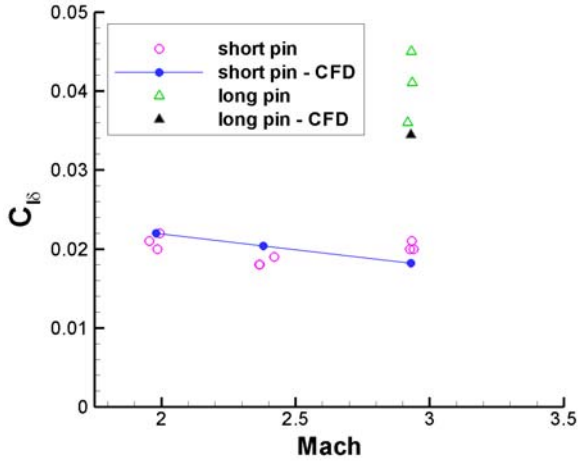

Fig. 17: Comparison of updated CFD to range test roll torque coefficient.

between Mach 2.0 and Mach 2.5 with a subsequent increase between Mach 2.5 and Mach 3.0. It is possible that a non-zero experimental angle-of-attack may be responsible for this discrepancy. For the long pin model, the CFD underpredicts $C_{l\delta}$. The scatter in the range test results suggests an angle-of-attack dependency supporting the hypothesis for the short pin discrepancy.

From CFD visualization, it is possible to see the forces created by the pins on the fins that are responsible for the roll torque (Fig. 18 and Fig. 19) If one also compares the shock structure predicted by the CFD (Fig. 20) to that seen in the range (Fig. 21) the similarities are easily noticeable. The small differences in the base flow are likely a result of differences in roll orientation, and hence the location of the control pin. Based on the comparison of the updated CFD results to the range data, CFD should be able to predict the forces produced by the control pins as the problem is varied (i.e. changes in pin shape, pin location, free stream Mach number).

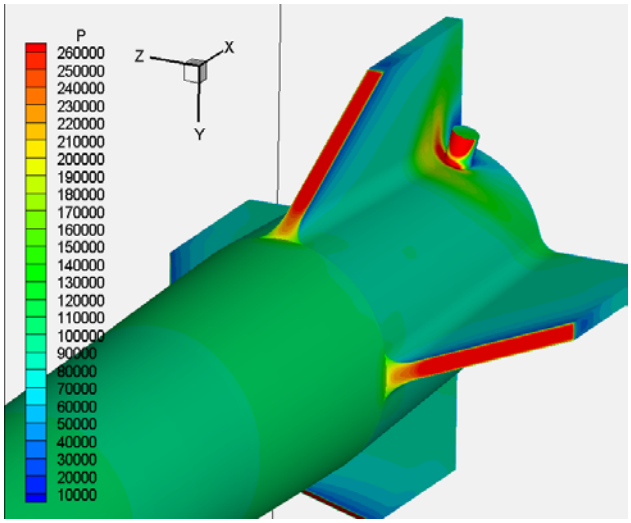

Fig. 18: Surface pressure contours for updated CFD on short pin model at Mach 2.93.

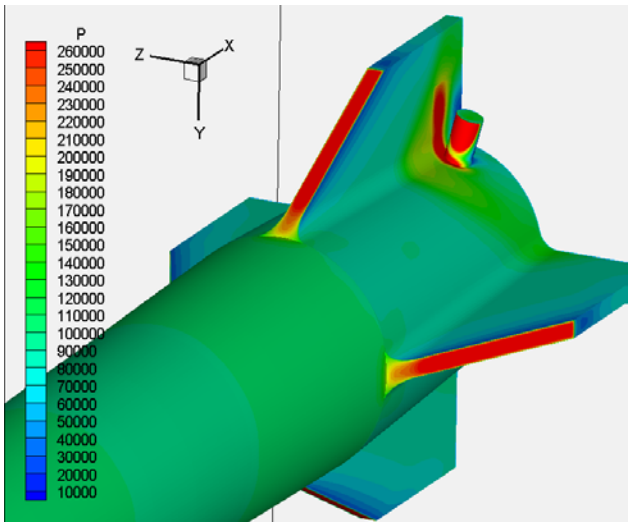

Fig. 19: Surface pressure contours for updated CFD on long pin model at Mach 2.93.

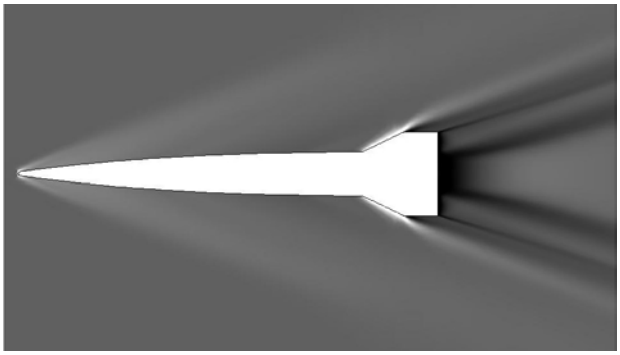

Fig. 20: Pressure coefficient contours through fin symmetry plane for short pin model at Mach 2.93.

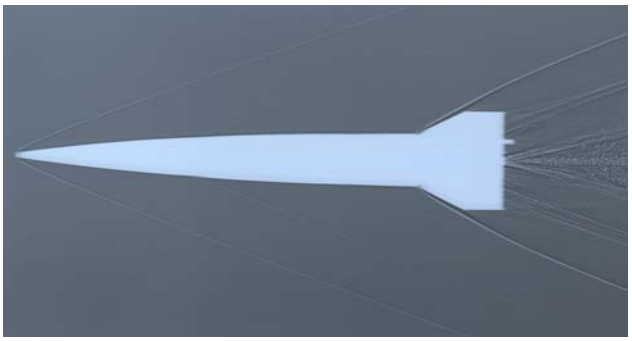

Fig. 21: Shadowgraph at station 27 for short pin model at Mach 2.93.

CONCLUSIONS

A complete validation program for the use of diametrically opposed pins to produce asymmetric lift was completed. Blind CFD calculations were performed to obtain C_{X0} and $C_{l\delta}$ over a large range of Mach numbers at 0° angle-of-attack for the GTRI optimized control pin configuration. The results of the CFD augmented previously obtained rifled test data. This augmented data was input into a database for use by the 6-DOF trajectory simulations to approximate the results of the range tests.

Flight hardware was designed and built with circular cross-section control pins for proof of concept. The flight test was completed and good quality spark shadowgraph photography for data reduction was obtained. Flight test analysis confirmed that the introduction of diametrically opposed control pins creates roll torque with an increase in drag. As expected, the longer control pin produced a greater amount of roll torque.

Comparison of the blind simulation results to the actual range data was quite good considering differences in geometry (nose, fins, control pins). This shows that 6-DOF tool in combination with the CFD provides an accurate prediction of the range performance, even when only a preliminary design is available, thereby enabling greater range safety and perhaps a smaller number of actual firings. When the exact geometry and flight conditions were simulated, agreement was quite remarkable. While the range tests were essential for concept validation, the agreement with CFD means the numerical solutions can be utilized to visualize the flow phenomena that could not otherwise be obtained or even investigate the effect of geometry changes on the flow prior to range testing.

This integrated approach has shown great promise for the optimization and strategic location of the control pins to achieve the turning force necessary to terminally steer a missile or projectile to its target, thereby increasing the lethality of future combat systems.

ACKNOWLEDGMENTS

The authors would like to acknowledge that funding for this project was provided by the DARPA Advanced Technology Office. This work was supported in part by a grant of computer time from the Department of Defense High Performance Computing Major Shared Resource Center at the U.S. Army Research Laboratory. The authors would like to thank Metacomp Technologies for providing the grid for the blind CFD and the results for the updated CFD. Finally, the authors would like to thank Dr. Peter Plostins for all his help and guidance with the range test and subsequent data reduction.

REFERENCES

ArrowTech Associates, 2001: Prodas 2000 Technical Manual, South Burlington, VT.

ArrowTech Associates, 1997: ARFDAS: Ballistic Range Data Analysis System, User and Technical Manual, South Burlington, VT.

Bornstein, J., Celmins, I., Plostins, P., and Schmidt, E.M., 1992: Launch Dynamics of Fin-Stabilized Projectiles, *J. of Spacecraft and Rockets*, **29**, **2**, 166-172.

Braun, W.F., 1958: The Free Flight Aerodynamics Range, BRL-R-1048, U.S. Army Ballistic Research Laboratory, Aberdeen Proving Ground, MD.

Goldberg, U.C., Peromian, O., and Chakravarthy, S., 1998: A Wall-Distance-Free K-E Model with Enhanced Near-Wall Treatment, *J. of Fluids Engineering*, **120**, **3**, 457-462.

Massey, K.C, McMichael, J., Warnock, T., and Hay, F., 2004: Design And Wind Tunnel Testing of Guidance Pins For Supersonic Projectiles, Army Science Conference, DO-01, 2004.

Metacomp Technologies, 2000: CFD++ User's Manual, Westlake Village, CA.

McCoy, R.L., 1999: Modern Exterior Ballistic: The Launch and Flight Dynamics of Symmetric Projectiles, Schiffer Military History, Atglen, PA, 308.

Plostins, P., Bornstein, J., and Celmins, I., 1991: The Effect of Sabot Wheelbase and Positions on the Launch Dynamics of Fin-Stabilized Kinetic Energy Ammunition, BRL-TR-3225, U.S. Army Ballistic Research laboratory, Aberdeen Proving Ground, MD.

Plostins, P., Celmins, I., Bornstein, J., and Deibler, J.E., 1989: The Effect of Front Borerider Stiffness on the Launch Dynamics of Fin-Stabilized Kinetic Energy Ammunition, BRL-TR-3057, U.S. Army Ballistic Research laboratory, Aberdeen Proving Ground, MD.

Silton, S, 2004: Comparison of Predicted Actuator Performance for Guidance of Supersonic Projectiles to Measured Range Data, AIAA-2004-5195, Aug. 2004.

Whyte, R., Hathaway, W., and Steinhoff, M., 2002: ARL-CR-501, U.S. Army Research Laboratory, Aberdeen Proving Ground, MD.

Weapons & Materials Research Directorate | Ballistics & Weapons Concepts Division

Integrated Numerical and Experimental Investigation of Actuator Performance for Guidance of Supersonic Projectiles

Dr. Sidra I Silton
U.S. Army Research Laboratory
&
Dr. Kevin C. Massey
Georgia Tech Research Institute

Army Science Conference
Orlando, FL
November 29 – December 2, 2004

Weapons & Materials Research Directorate | Ballistics & Weapons Concepts Division

Objectives

- Conduct developmental testing on DARPA command-guided, medium caliber projectile program
- Model and validate placement of control pin next to fin produces asymmetric lift
  - GTRI found shock patterns created
  - Impinge on fin and body surfaces
- Determine if 2 diametrically placed control pins can be used to create roll torque
  - Complete high performance computations to predict projectile behavior
  - Conduct an experimental range program to determine the asymmetric lift produced
  - Compare the computational and experimental results for future use

Blind Simulations

- Completed prior to experimental range test
  - Determine expected flight characteristics of projectile
- Two part
  - Computational fluid dynamics (CFD)
    - » CFD++
    - » Full scale model
  - Six degree-of-freedom (6-DOF) simulations
    - » PRODAS

Blind CFD Simulations

- CFD++ Code
  - 3D Reynolds Averaged Navier-Stokes (RANS) Solver
  - Pointwise k-ε turbulence model
  - Finite-volume framework
  - Up to second order spatial accuracy
  - Point-implicit integration to solve steady-state simulation
- Full scale models
  - 50mm fin span
  - Fin leading and trailing edges tapered
  - Modeled with and without control pins
    - » Rectangular and trapezoidal control pins
      - original GTRI configuration (patent pending)

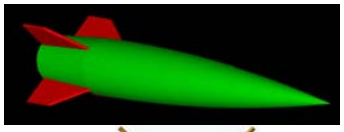

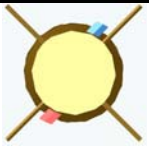

Blind CFD Simulations (cont.)

- Grid obtained from Metacomp Technology
  - Unstructured grid
    - » Hexahedral with some triangular prisms
    - » Approximately 2.9 million cells
- Force and Moment Data
    - » Mach 1.5 to Mach 4.0
    - » 0° angle-of-attack
    - » Change in drag due to presence of control pins
    - » Roll torque induced by control pins

CFD Drag Coefficient Comparison

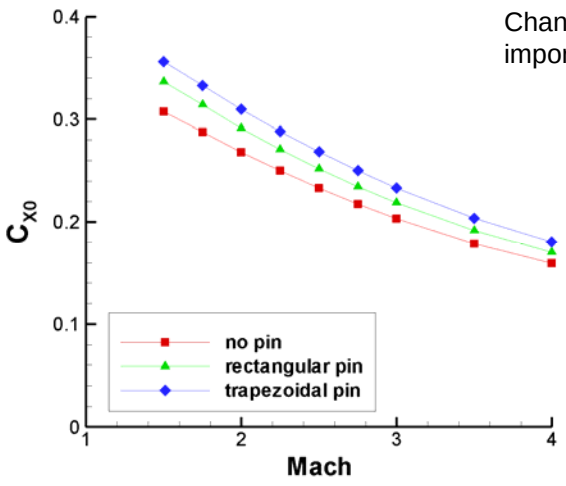

Change in C_{X0} of primary importance

CFD Roll Torque

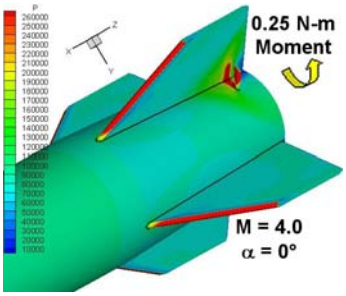

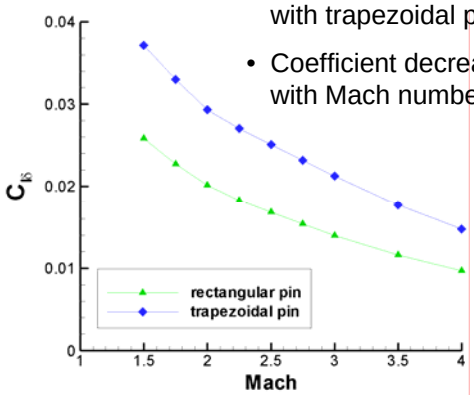

- Greater torque expected with trapezoidal pin
- Coefficient decreases with Mach number

Blind 6-DOF Simulations

- PRODAS 6-DOF fixed plane trajectory simulation
  - Physical characteristics specified
    - » From previous baseline experimental results
  - 4th order Runge-Kutta numerical integration scheme
    - » Time step dynamically chosen to account for pitch frequencies
  - Database of aerodynamic coefficients as function of Mach number
- Aerodynamic coefficient database
  - Utilized previous baseline experimental results as determined by ArrowTech Associates
    - » Rifled barrel test
    - » No control pins
    - » Blunt fin leading and trailing edges
    - » Static and dynamic aerodynamic coefficients determined
  - Modified coefficients based on CFD results of rectangular pin
    - » Introduced roll torque coefficients
    - » Modified C_D to account for increased drag

Blind 6DOF Simulations (cont.)

- "Flew" projectile under expected launch conditions of new range tests
  - Smooth bore gun
  - Mach 2.0, 2.5, 3.0
  - Sea level meteorological conditions
  - Initial yaw rate of –15 rad/sec
  - 0.001° elevation, no azimuth
- Determine roll characteristics of new range test
  - Number of turns expected over length of range
    - » Enough turns expected in order to be observed
  - Mach number dependency
  - Steady-state roll

6DOF Revolution Prediction

Rectangular Pins

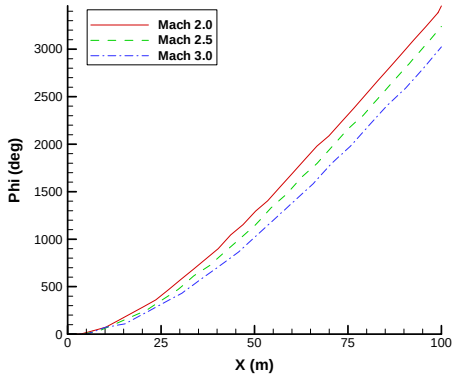

- 8 – 10 turns expected depending on Mach number

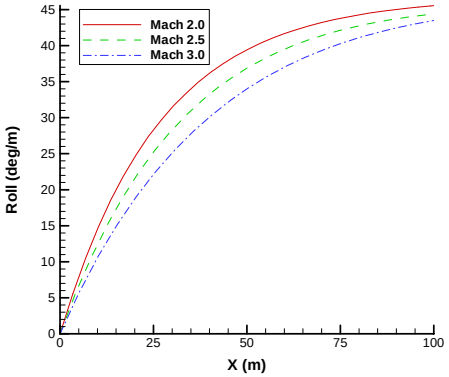

- Near steady-state roll rate may be reached by end of range

Current Experimental Test

- Range
  - ARL Aerodaynamics Range
    - » 100m in length
  - Orthogonal x-rays to ensure structural integrity
  - Orthogonal spark shadowgraph photography
    - » 5 groups of stations
    - » Over entire length of range
    - » Extract data from film for use with range reduction software
  - Modified 25mm Bushmaster Mann Barrel used
    - » Smooth bore barrel

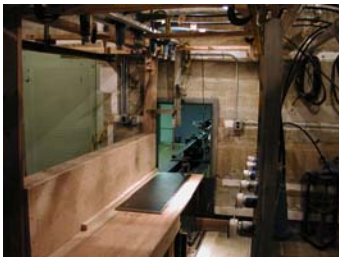

Current Test
Projectile

- Same basic shape as previous rifled test for consistency
  - Sub-scale 25mm fin span
  - CG shifted for stability
    - » Tungsten nose
    - » Aluminum body (hollowed out) and fins
  - Blunt fin leading and trailing edges
  - Spin pin inserted in projectile base
    - » Used to determine projectile roll position
- 3 configurations tested
  - No control pins (baseline)
  - 0.07” length control pins (short)
    - » Length equivalent to that used in blind CFD/6-DOF
  - 0.10” length control pins (long)
- Diametrically opposed control pins inserted to generate roll
  - Steel - 1/16” Circular cross-section
    - » Ease of machining to establish concept

Short pin model

Long pin model

Current Test
Sabot System

- 3 piece system designed for use with smooth bore gun
  - 4 nylon sabot petals
  - Nylon pusher cup
  - Steel pusher

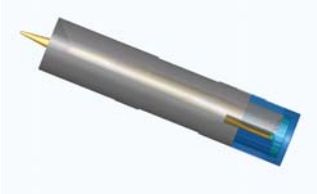

3-D rendering

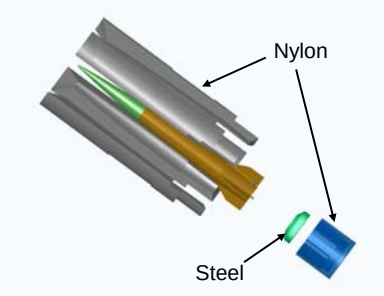

3-D rendering – Exploded View

Current Test
Miscellaneous

- Gun launch
  - Structural integrity maintained
  - Up to 3 Mach numbers investigated
    - » Baseline – Mach 3.0, 2.5, 2.0 (1 each)
    - » Short – Mach 3.0, 2.5, 2.0 (3 each)
    - » Long – Mach 3.0 (3 each)
- Range Reduction
  - Horizontal and vertical film utilized at each station
    - » Accurately determine projectile orientation
      - X, Y, Z
      - Pitch, Roll, Yaw
  - ARFDAS
    - » Post-processing of data read from spark shadowgraphs
    - » Completes 6DOF fit of range data
  - Aerodynamic coefficients determined

Axial Force Coefficient

- Axial Force
  - Decreases with increasing Mach number
    - » Nearly linear
  - For a given Mach number
    - » Increases with introduction of control pin
    - » Increases with increase in control pin length
  - CFD under predicts axial force
    - » Both baseline and with pin
      - CFD has fin leading and trailing edges tapered
    - » Increase in force due to presence of control pin under predicted as well
    - » Augment rifled data agrees well

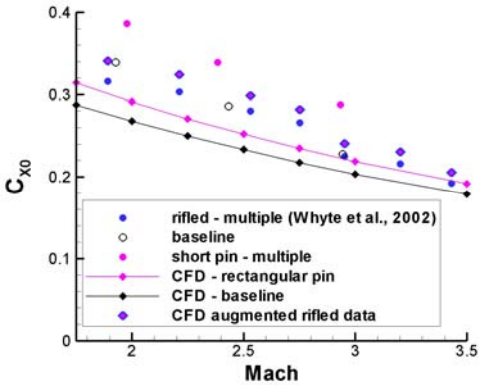

Roll Torque Development

- Roll Torque
  - Diametrically opposed placement of control pins creates roll torque
  - 50% increase in control pin length nearly doubles roll torque
    - » Expect twice as many rotations during range travel
  - Experimental data does not vary significantly with Mach number
  - Comparison to CFD prediction
    - » Good agreement at Mach 2.0 and 2.5
      - 3-D relieving effects significant
      - Control pin differences insignificant
    - » CFD over predicts at Mach 3.0
      - Shock structure likely different due to difference in pin shape

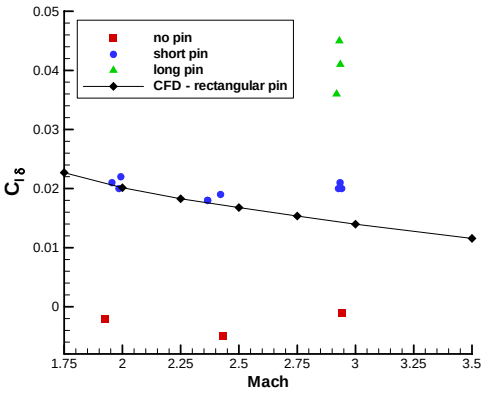

Current Test
Spark Shadowgraphs

Shot 24096 – Mach 3.0 short pin

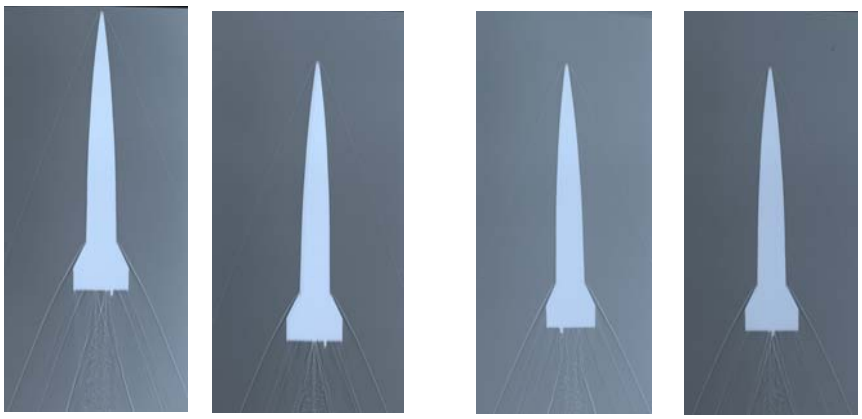

22v ***27v*** ***295h*** ***300h***

Little change in spin pin location → little/slow roll

Greater change in spin pin location → faster roll

Roll Rate

- Roll Rate
  - Longer Pin generates greater roll as expected
  - Fairly good agreement between range test 6DOF fit and predicted 6DOF
    - » Differences likely due to differences in pin shape
      - 6DOF over predicts at Mach 2.0 and 2.5
      - 6DOF under predicts at Mach 3.0

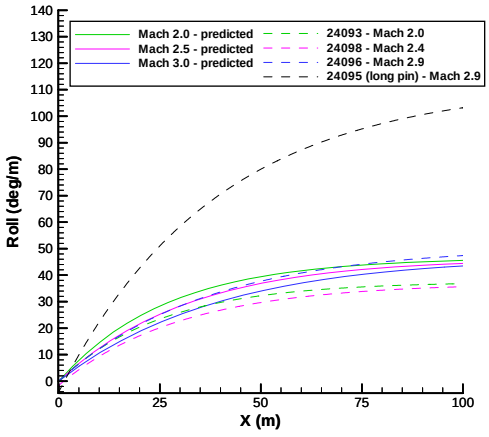

Revolutions

- Number of Revolutions
  - Long Control pin causes approximately twice as many revolutions as short control pin
  - Range tests show increase in number of revolutions with Mach number
    - » Simulations predicted a decrease
      - Differences in $C_{l\delta}$, C_{lp}, C_{X0}
  - Preliminary simulations predict magnitude of number of revolutions fairly well

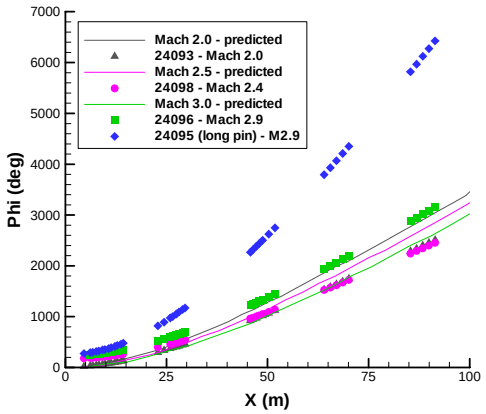

Updated 6-DOF

- Used coefficients determined in range reduction
  - Confirm accuracy of simulations
    - » Initial roll rate in simulation not adjusted to match range tests
    - » Offset simulations results by initial experimental Phi value

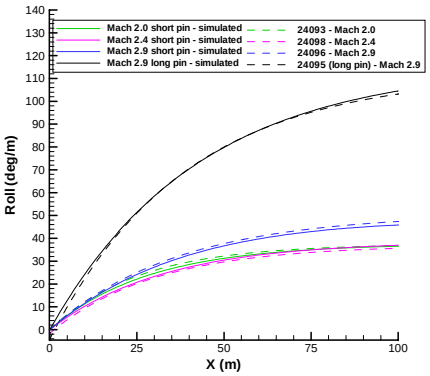

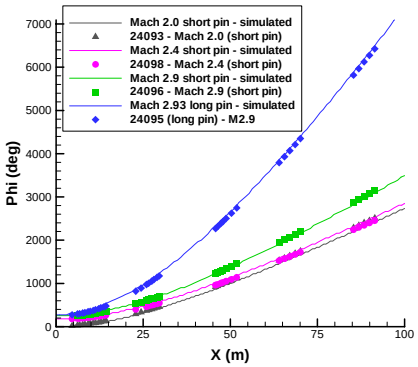

Updated CFD

- Completed after conclusion of range test
  - 2 models
    - » Geometric shape and dimensions of short, cylindrical pin model
    - » Geometric shape and dimensions of long, cylindrical pin model
  - Matched average range conditions
    - » 0° angle of attack
    - » Investigated each average Mach number from range
      - Short pin – Mach 2.0, 2.5, 3.0
      - Long pin – Mach 3.0
  - Completed by Metacomp Technologies
    - » Data provided through GTRI

Updated CFD

C_{X0} and $C_{l\delta}$

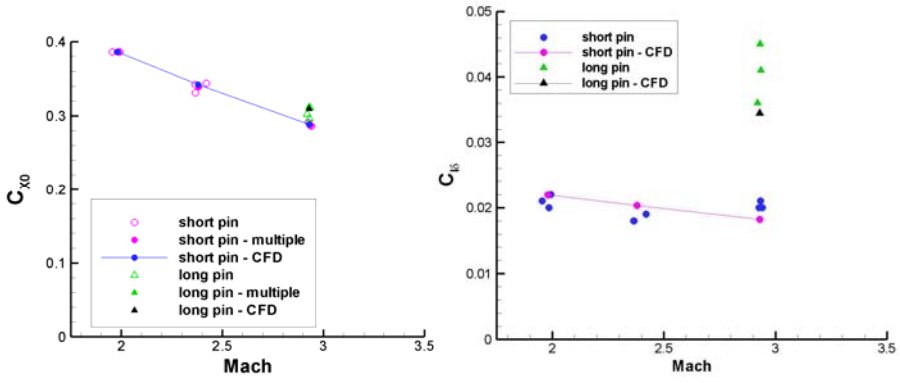

Updated CFD
Pressure Contours

Weapons & Materials Research Directorate *Ballistics & Weapons Concepts Division*

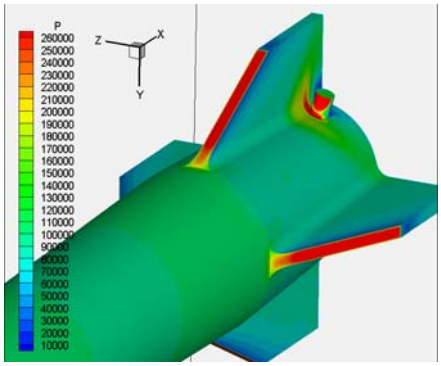

Short cylindrical control pin

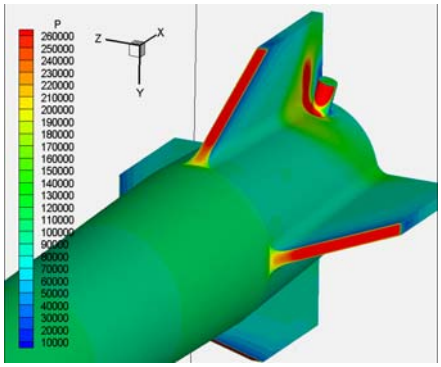

Long cylindrical control pin

Updated CFD

Weapons & Materials Research Directorate *Ballistics & Weapons Concepts Division*

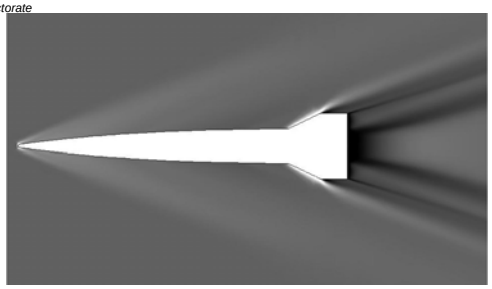

CFD Pressure Contours

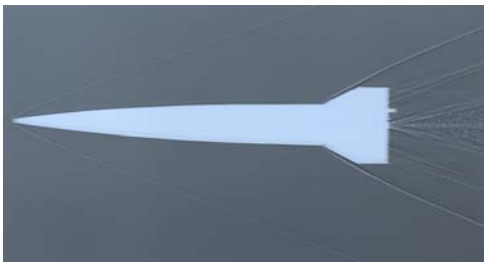

Range Shadowgraph

Summary

- Blind Simulations Performed
  - CFD used to obtain force and moment data over large range of Mach numbers with no angle-of-attack
    - » Utilized GTRI optimized control pin configuration
  - Completed six degree of freedom trajectory simulations
    - » Used CFD data augment previously obtained test data on baseline shape
    - » Determined how projectile could be expected to behave during range test
- Completed the flight test
  - Circular cross-section control pins used
  - 15 rounds successfully launched and analyzed
  - Confirmed introduction of diametrically opposed control pins created roll torque

Summary (cont.)

- Results of blind simulations compared favorably to experimental results
  - Many assumptions made
    - » Rifled test data augmented
  - Geometric differences
    - » Nose, fins, control pin
- Updated CFD and 6-DOF results agreed remarkably well with experimental data
  - Exact geometry and flight conditions matched
  - Implies numerical solutions can be used to
    - » Visualize otherwise unobtainable flow phenomena
- CFD in conjunction with 6-DOF simulations can be used to predict range performance
  - Greater range safety
    - » even if only preliminary design is available
    - » Investigate affects of geometry changes on flow prior to range testing
  - Smaller number of actual firings

Acknowlegdements

- Funding for this project was provided by the DARPA Advanced Technology Office.
- This work was supported in part by a grant of computer time from the Department of Defense High Performance Computing Major Shared Resource Center at the U.S. Army Research Laboratory.
- Metacomp Technologies provided the grid for the blind computations and the data for the updated CFD comparisons.
- Dr. Peter Plostins for all his help and guidance with the range test and subsequent data reduction.